Publications of the Astronomical Society of Japan Advance Access published October 12, 2015

Publ. Astron. Soc. Japan (2015) 00 (0), 1–9
doi: 10.1093/pasj/psv092
Advance Access Publication Date: 2015 0

1SWASP J075102.16+342405.3: a deep overcontact binary system with a period under the short period cut-off

Linqiao Jiang,[1,*] Shengbang Qian,[2,3,4] Jia Zhang,[2,3] and Nianping Liu[2,3]

[1]Department of Physics, School of Science, Sichuan University of Science & Engineering, Zigong, 643000, China
[2]Yunnan Observatories, Chinese Academy of Sciences, PO Box 110, 650011 Kunming, China
[3]Key Laboratory of the Structure and Evolution of Celestial Objects, Chinese Academy of Sciences, PO Box 110, 650011 Kunming, China
[4]Graduate University of the Chinese Academy of Sciences, Yuquan Road 19, Sijingshang Block, 100049 Beijing City, China

*E-mail: linqiao@ynao.ac.cn

Received 2015 March 6; Accepted 2015 August 31

Abstract

New photometry of two different seasons for the extremely short period eclipsing binary 1SWASP J075102.16+342405.3 were performed. The two sets of derived light curves show a large difference in their shape, i.e., the 2013 light curves show big asymmetry, whereas the 2014 light curve is almost symmetric. All light curves were analysed using the 2013 version of the Wilson–Devinney (W-D) code. The obtained solutions show that 1SWASP J075102.16+342405.3 is of the A subtype W UMa contact system with an extremely high fill-out of $f \approx 96\%$ and a high mass ratio of 0.70–0.78. Furthermore, a third light contributing to the total flux of the system was found. All these properties make the system a very special short-period source. The analysis of the 2013 light curves proved that the changes in the light curve shape are caused by magnetic activities. By means of all available times of minimum light, the variation of the orbital period was studied. It was found that the $O - C$ diagram implies an increasing orbital period over a time span of eight years, which may be caused by the mass transfer from the less massive component to the more massive one; however, we are more inclined to say that it is only a part of a long period cyclic variation which can be explained by the light-travel time effect (LTTE) via the third body.

Key words: binaries: close — binaries: eclipsing — stars: individual (1SWASP J075102.16+342405.3)

1 Introduction

It was previously shown that the period distribution of contact binaries exhibits a sharp short-period limit at about 0.22 days (Rucinski 1992, 2007). The scarcity of such extremely short-period contact systems could be explained by the following reasons: (1) the dynamically stable contact systems cannot exist with effective temperatures lower than the full-convection point (Rucinski 1992); (2) as the timescales of the angular momentum loss are much longer, binaries with less-massive primaries have not yet had time to reach Roche lobe overflows even within the age of the universe (Stępień 2006, 2011); (3) the mass transfer

for low-mass contact binaries is so unstable that these systems are destroyed on a quite short timescale (Jiang et al. 2012); (4) due to their faintness, they are still very difficult to detect. Thanks to the efforts of several international surveys [e.g., Sloan Digital Sky Survey (SDSS), WFCAM Transit Survey, and SuperWASP], a number of eclipsing binary candidates with periods under the limit ($P < 0.22$ d) can now be discovered. Observations and investigations of such short-period close binaries can provide valuable information on the formation and evolution of contact binaries as well as shed light on the contributing factors behind the scarcity of contact binaries below the short-period limit (Qian et al. 2014).

The system 1SWASP J075102.16+342405.3 (hereafter J075102) was found to be a newly discovered eclipsing binary candidate by Lohr et al. (2013a), who used the SuperWASP archive of ~30 million objects to search for and analyse main sequence eclipsing binaries with very short orbital periods (<2000 s or ~0.2315 d). According to Lohr et al. (2013a), J075102 has a short period of 18072.478 s, light curves typical of EW types, and minima which are nearly equal (with a difference of only 0.03 mag between the primary and secondary depths). All these features signify that J075102 is probably a new contact binary with a period under the sharp period cut-off, therefore, J075102 was placed into our observational queue. In this paper, the complete R_cI_c light curves are presented and analyzed with the 2013 version of the W-D code. The first photometric solutions of the system are derived. In addition, the variations in the orbital period are analyzed based on all available light minima, and a brief discussion of our results is presented in the last section.

2 New photometric observations

R_c- and I_c-band observations of J075102 were carried out on 2013 January 8 and 16 with the PI 512 × 512 TE CCD photometric system attached to the 85 cm telescope at the Xinglong Station of the National Astronomical Observatories of China. The integration times of each image for the R_c and I_c filters were 30 s and 20 s, respectively. One of the CCD images obtained by the 85 cm telescope is shown in the upper left-hand panel of figure 1. Afterwards, we re-observed the system on 2014 January 10 with the PI 1274 × 1152 TE CCD55-30-1-348 photometric system attached to the 2.16 m telescope of the Xinglong Station, with exposure times of 25 s for the R_c band. One of the CCD images obtained in this observation is shown in the upper right-hand panel of figure 1. As shown in the upper panel of figure 1, the objects marked "V" in both pictures represent our target star J075102. The aperture photometry package PHOT (which measures magnitudes for a list of stars) of IRAF was used to reduce all the observed images. Another two stars, GSC 2475−0659 ($\alpha_{J2000.0} = 07^h51^m08^s.88$, $\delta_{J2000.0} = +34^\circ22'40''.3$) and GSC 2475−0631 ($\alpha_{J2000.0} = 07^h51^m07^s.57$, $\delta_{J2000.0} = +34^\circ22'43''.1$), which are respectively marked as "C" and "CH" in figure 1, were chosen as the comparison star and the check star, respectively.

The lower left-hand panel of figure 1 shows a CCD image of J075102 obtained from the SDSS dr7. It can be clearly seen that the target J075102 is actually a visual binary, while the images obtained by the 85 cm and 2.16 m telescopes cannot resolve them due to lower resolution. In consideration of this situation, we can only measure the two neighbors as a single star by setting a larger photometric aperture. Meanwhile this behooves us to ask following question: which one of the two neighbors is the variable star? Fortunately, apart from the previous two photometric observations, four extra minimum light observations were performed using the DW436 2048 × 2048 CCD photometric system attached to the 1 m reflecting telescope at the Yunnan Observatories. During one of the light minima observations on 2014 December 23, the atmospheric seeing conditions were very good. The lower right-hand panel of figure 1 shows one of the CCD images obtained on that day, where one can distinguish the two neighbors easily. According to this minimum light observation, we identified that the brighter star of the two neighbors is our target J075102, and that the other one is an invariable visual companion. J075102 and the visual companion were marked as "V" and "vc" in the lower panel of figure 1, respectively.

The phased light curves from the 85 cm and 2.16 m telescopes are displayed in figure 2. As one can see, the shape of the light curves has changed dramatically over a span of just one year. The two light curves in 2013 show a high degree of asymmetry, namely, the primary maximum (phase 0.25) is significantly higher than the secondary one (phase 0.75), while the light curve in 2014 is nearly symmetric. This variability of shape of the light curves may be caused by the star's magnetic activities.

3 Orbital period variations

Though Lohr et al. (2013a) has given the $O - C$ diagrams of J075102, due to the time span of the observations not being long (only about three years), the obtained $O - C$ curve showed no significant period change. Fortunately, those useful eclipse timings were sent to us by Dr. Marcus Lohr. Combined with our six photometric observations, by using a least-squares parabolic fitting method, a total of eight times of minimum light were determined, which are listed in table 1.

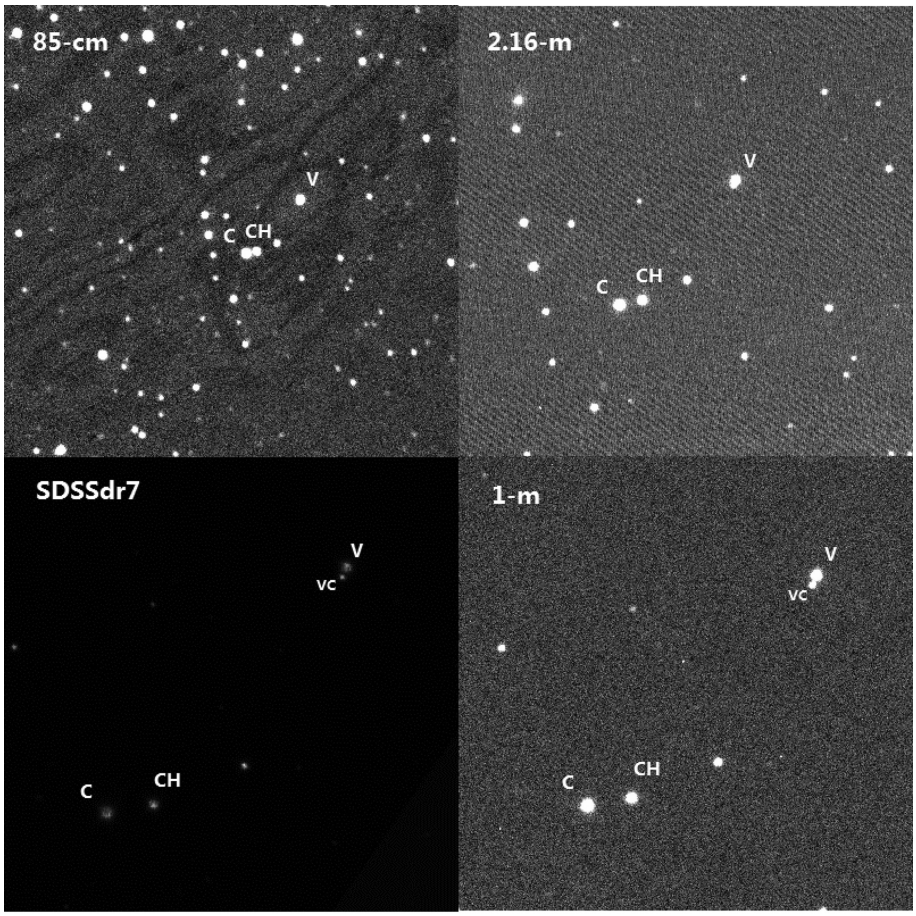

Fig. 1. Upper left-hand panel: One of the I_c-band CCD images obtained with the 85 cm telescope. Upper right-hand panel: One of the R_c-band images obtained with the 2.16 m telescope. Lower left-hand panel: *i*-band optical image from SDSSdr7 of SkyView. Lower right-hand panel: One of the CCD images obtained with the 1 m telescope. The marks "V", "vc", "C", and "CH" stand for our target J075102, the invariable visual companion, the comparison star, and the check star, respectively.

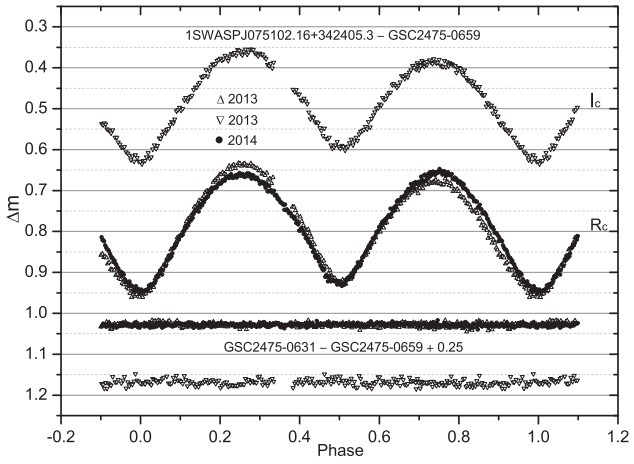

Fig. 2. The phased light curves of J075102. Different symbols stand for light curves in different seasons. The magnitude differences between the check star and the comparison star are also shown in the lower part.

Using the following ephemeris:

$$\text{Min. I(HJD)} = 2456668.071445 + 0^{\text{d}}.20917233 \times E, \quad (1)$$

where 2456668.071445 is one of the times of minimum light listed in table 1, and $0^{\text{d}}.20917233$ was determined by Lohr et al. (2013a), the $(O - C)$ values for all the eclipsing times were calculated and plotted in the upper panel of figure 3. Regarding figure 3, two things need to be noted. First, one data point from the SuperWASP data was not used here due to its large deviation from other points. Secondly, as shown in the figure 3, the two filled square points, computed with the two times of minimum light occurring at HJD 245609 in table 1, show a large $O - C$ difference that is much greater than their errors. This is because the lower filled square point is calculated from light curves of a high degree of asymmetry; its systematic errors are far greater than the random fitting errors. However, the two filled square points were retained since they do not alter the trend of the $O - C$ curve.

Table 1. New times of minimum light of J075102.*

Date	HJD	Error	Min type†	Filter‡	Telescope
2013 Jan 16	2456309.128828	0.000266	I	R_cI_c mean	85 cm
2013 Jan 16	2456309.235917	0.000271	II	R_cI_c mean	85 cm
2014 Jan 10	2456668.071445	0.000150	I	R_c	2.16 m
2014 Jan 10	2456668.176110	0.000145	II	R_c	2.16 m
2014 Mar 03	2456720.155766	0.000500	I	R_cI_c mean	1 m
2014 Dec 05	2456997.309610	0.000483	I	N	1 m
2014 Dec 20	2457012.369896	0.000538	I	N	1 m
2014 Dec 23	2457015.298091	0.000370	II	N	1 m

*The errors quoted in the third column are estimated random errors, and that the systematic errors may be much larger due to the asymmetric light curves.
†I and II refers to the primary minimum and secondary minimum, respectively.
‡"N" means no filters were used.

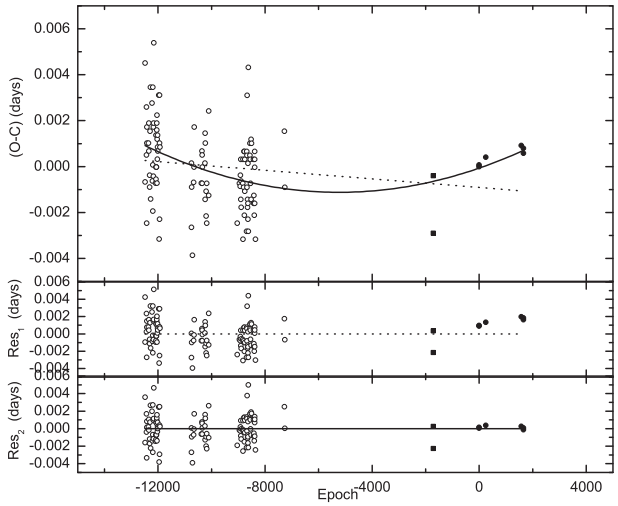

Fig. 3. Upper panel: $O - C$ curve calculated with the linear ephemeris equation (1). The dotted line represents a linear fit, while the solid line represents an upward parabolic variation. The open circles stand for the SuperWASP data, the filled points represent the new times of table 1. Middle panel: the residuals from the linear fit. Lower panel: Residuals for the upward parabolic variation.

Then, a linear fit (dotted line in the upper panel of figure 3) yielded a revised ephemeris as below:

$$\text{Min. I(HJD)} = 2456668.070533 + 0^{\text{d}}.20917224 \times E, \quad (2)$$

where 2456668.070533 and $0^{\text{d}}.20917224$ are the revised initial epoch and orbital period, respectively. The corresponding fitting residuals are displayed in the middle panel of figure 3. As shown in this panel, some points are not fitted well. With this in mind, a quadratic fit (solid line in the upper panel of figure 3) was used. The following ephemeris was derived by using a least-squares solution:

$$\begin{aligned}\text{Min. I} = {} & 2456668.07138(\pm 0.00053) \\ & + 0^{\text{d}}.20917273(\pm 0.00000014) \times E \\ & + 3.86(\pm 0.98) \times 10^{-11} \times E^2. \end{aligned} \quad (3)$$

The residuals left after removing the upward parabolic change are plotted in the lower panel of figure 3. Comparing this with the middle panel, though the additional quadratic term provides a better fit than a simple linear correction, it is necessary to prove that the reduction in residual scatter merits the increased model complexity. To see whether the linear model is adequate, we use the ANOVA-type formula

$$F = \frac{[SSE(LM) - SSE(PM)]/[N(PM) - N(LM)]}{SSE(PM)/[n - N(PM)]}, \quad (4)$$

where $SSE(LM)$ and $SSE(PM)$ are the sum of squared residuals with the linear model and the parabolic model, $N(LM)$ and $N(PM)$ are the number of regression parameters, and n is the sample size. The observed value F is 15.64, larger than the appropriate critical value $F_{0.01}(1,\ 120) = 6.85$, which suggests that the linear model should be rejected. The quadratic term in equation (3) reveals a period increase at a rate of $dP/dt = +1.35(\pm 0.35) \times 10^{-7}$ d yr^{-1}.

4 The analysis of the light curves using the W-D code

In the present paper, the photometric observations of J075102 were analysed by using the 2013 version of the W-D program (Wilson & Devinney 1971; Wilson 1979, 1990; Van Hamme & Wilson 2007; Wilson 2008; Wilson et al. 2010; Wilson 2012). Before the analysis, we need to estimate the temperature of the primary component. By using the USNO-B1.0 Catalog measurements of $R_1 = 13.22$, $R_2 = 13.47$, and $I = 12.57$ from the VizieR database, the color indices $R_1 - I = 0.65$ and $R_2 - I = 0.90$ were obtained, which corresponds to a spectral type of about K5–K9 (Cox 2000). Therefore the temperature should be between 3800 and 4400 K, and we consequently set $T_1 = 3950^{+450}_{-150}$ K as the temperature of primary star. Considering the high degree of asymmetry in the 2013 light curves, the basic parameters of the system were

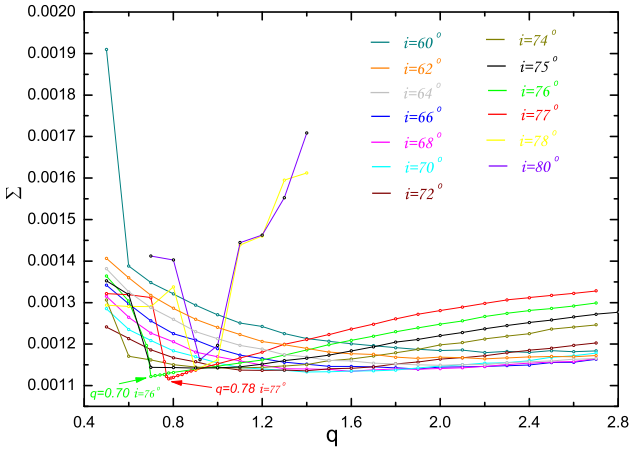

Fig. 4. The Σ to q diagram; different colors stand for different orbital inclinations. (Color online)

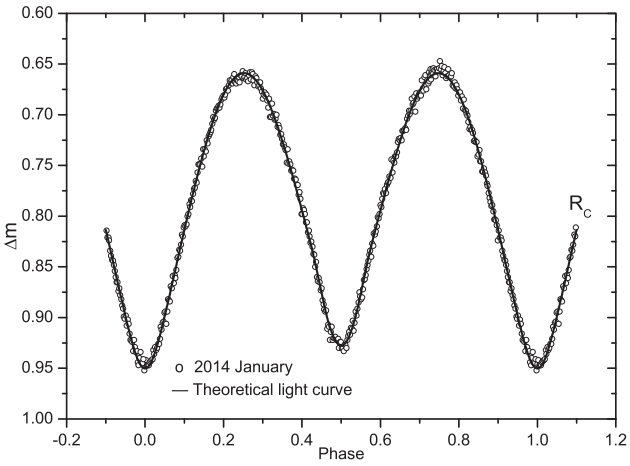

Fig. 5. The observed (in 2014 January) and theoretical light curves (solid line) of J075102.

obtained by the analysis of the 2014 light curve, and then applied to the high asymmetry light curves in 2013. The following atmospheric parameters were adopted in the analysis: the bolometric albedos $A_1 = A_2 = 0.5$ and the gravity-darkening coefficient $g_1 = g_2 = 0.32$. For the bolometric and bandpass limb-darkening coefficients, an internal computation with the logarithmic law was used. Different modes were tried (Modes 2, 3, 4, and 5 correspond to the scenarios in which the binary components are detached, over-contact, semi-detached with star 1 accurately filling its limiting lobe, and semi-detached with star 2 precisely filling its limiting lobe, respectively), and the solutions converged at mode 3 only.

To get reliable solutions, an i–q search method was used during the analysis. For a start, we varied the orbital inclination from 60° to 80° with a step length of 2°, varied the mass ratio from 0.5 to 2.7 with a step length of 0.1, and set the remaining parameters (T_2: the temperature of star 2, Ω_1: the dimensionless potential of star 1, L_{1R_c}: the monochromatic luminosity, and l_{3R_c}: the bandpass third light) as adjustable. For each combination of orbital inclination and mass ratio, the convergent solutions were derived by an iteration process. The relations between the resulting sum of the weighted square deviations Σ and mass ratio q are plotted in figure 4, where it can be seen that the best-fitting solution was achieved at $q = 0.70$ and $i = 76°$. To be confident, the step sizes around the minimum were set to 1° in orbital inclination and 0.02 in mass ratio. As shown in figure 4, the smaller step size yielded another best-fitting solution, which was achieved at $q = 0.78$ and $i = 77°$. Since these two solutions, $q = 0.70$ and $i = 76°$, and $q = 0.78$ and $i = 77°$, were achieved with a similar Σ, and fit the observations in 2014 almost equally well, both of them were adopted in this paper. All the solutions from observations in 2014 are summarized in table 2. The corresponding theoretical light curve is plotted in figure 5. As shown in this

Table 2. Photometric solutions for observations in 2014.

Parameters	$T_1 = 3950$ [K]		$T_1 = 3800$ [K]		$T_1 = 4400$ [K]	
i [°]	76	77	76	77	76	77
q (m_2/m_1)	0.70	0.78	0.70	0.78	0.70	0.78
T_2 [K]	3902	3876	3742	3716	4334	4308
$\Omega_1 = \Omega_2$	2.857	2.962	2.857	2.961	2.857	2.961
$L_1/L_{total}(R_c)$ [%]	22.9	21.8	23.3	22.3	23.3	22.1
$L_3/L_{total}(R_c)$ [%]	60.8	62.2	60.6	62.0	60.1	61.5
r_1 (pole)	0.452	0.446	0.451	0.445	0.451	0.444
r_1 (side)	0.497	0.490	0.495	0.488	0.495	0.487
r_1 (back)	0.586	0.589	0.582	0.586	0.581	0.584
r_2 (pole)	0.394	0.405	0.394	0.405	0.394	0.405
r_2 (side)	0.429	0.443	0.429	0.443	0.429	0.443
r_2 (back)	0.578	0.589	0.578	0.589	0.578	0.589
f (the degree of contact)	96.2%	95.6%	96.3%	95.6%	96.3%	95.6%
Σres^2	0.00112	0.00112	0.00126	0.00128	0.00116	0.00113

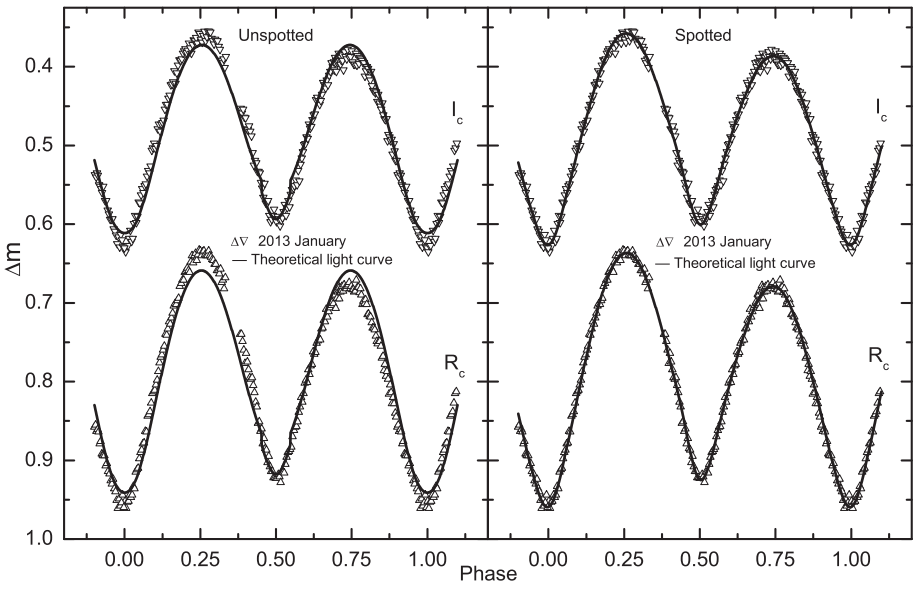

Fig. 6. Left-hand panel: the observed (in 2013 January) and theoretical light curves (solid line) of J075102 calculated without spotted models. Right-hand panel: the same as the left-hand panel but calculated with spotted models.

Table 3. Photometric solutions for observations in 2013.

Parameters	$T_1 = 3950$ [K]		$T_1 = 3800$ [K]		$T_1 = 4400$ [K]	
i [°]	76	77	76	77	76	77
q (m_2/m_1)	0.70	0.78	0.70	0.78	0.70	0.78
T_2 [K]	3902	3876	3755	3724	4313	4286
$\Omega_1 = \Omega_2$	2.858	2.960	2.857	2.950	2.855	2.954
$L_1/L_{\rm total}(R_{\rm c})$ [%]	22.9	21.9	23.0	21.8	23.9	22.5
$L_1/L_{\rm total}(I_{\rm c})$ [%]	20.7	19.8	20.8	19.6	21.4	20.1
$L_3/L_{\rm total}(R_{\rm c})$ [%]	60.7	62.0	60.7	62.5	59.6	61.2
$L_3/L_{\rm total}(I_{\rm c})$ [%]	64.2	65.3	64.2	65.8	63.5	65.0
r_1 (pole)	0.451	0.445	0.451	0.447	0.451	0.446
r_1 (side)	0.495	0.489	0.495	0.491	0.495	0.490
r_1 (back)	0.581	0.587	0.581	0.594	0.583	0.591
r_2 (pole)	0.394	0.406	0.394	0.408	0.395	0.407
r_2 (side)	0.429	0.443	0.429	0.446	0.430	0.445
r_2 (back)	0.577	0.592	0.577	0.613	0.582	0.602
f (the degree of contact)	96.2%	95.6%	96.1%	96.8%	98.1%	97.2%
$\theta_{\rm s}$[°]*	106.0	103.7	99.3	102.3	106.4	105.8
$\psi_{\rm s}$[°]*	15.9	15.9	13.2	13.7	10.2	11.2
$r_{\rm s}$[°]*	45.53	45.53	42.64	44.35	41.63	43.04
$T_{\rm s}/T$*	0.934	0.934	0.928	0.924	0.869	0.879
$\theta_{\rm s}$[°]†	63.7	63.8	63.8	64.2	63.7	64.9
$\psi_{\rm s}$[°]†	17.0	17.0	15.8	16.1	16.4	16.0
$r_{\rm s}$[°]†	16.29	16.29	16.80	17.34	12.39	13.49
$T_{\rm s}/T$†	1.320	1.320	1.310	1.302	1.584	1.554
Σres^2	0.00124	0.00124	0.00134	0.00134	0.00125	0.00124

*"dark spot" on the primary star.
†"hot spot" on the secondary star.

figure, those parameters model the observations made in 2014 very well.

Then the six sets of photometric parameters listed in table 2 were used as starting points in the analysis of the 2013 light curves. Differential corrections were performed many times until it converged, resulting in the final solutions. The theoretical light curves computed with these photometric elements are plotted in the left-hand panel of

Table 4. Photometric solutions of J075102.

Parameters	Light curve of 2014		Light curves of 2013	
i [°]	76	77	76	77
q (m_2/m_1)	0.70	0.78	0.70	0.78
T_1 [K]	3300	3300	3300	3300
T_2 [K]	3242	3217	3252	3224
$\Omega_1 = \Omega_2$	2.857	2.962	2.856	2.949
$L_1/L_{\rm total}(R_{\rm c})$ [%]	24.0	22.8	23.2	21.8
$L_1/L_{\rm total}(I_{\rm c})$ [%]	–	–	21.1	19.7
$L_3/L_{\rm total}(R_{\rm c})$ [%]	59.3	60.7	60.4	62.2
$L_3/L_{\rm total}(I_{\rm c})$ [%]	–	–	63.8	65.5
r_1 (pole)	0.451	0.445	0.451	0.447
r_1 (side)	0.495	0.488	0.495	0.492
r_1 (back)	0.582	0.586	0.582	0.595
r_2 (pole)	0.394	0.405	0.394	0.408
r_2 (side)	0.429	0.442	0.430	0.446
r_2 (back)	0.578	0.589	0.580	0.616
f (the degree of contact)	96.2%	95.4%	96.4%	98.4%
$\theta_{\rm s}$ [°]*	–	–	103.0	102.2
$\psi_{\rm s}$ [°]*	–	–	14.4	13.6
$r_{\rm s}$ [°]*	–	–	42.89	44.19
$T_{\rm s}/T$*	–	–	0.928	0.924
$\theta_{\rm s}$ [°]†	–	–	71.7	74.0
$\psi_{\rm s}$ [°]†	–	–	8.8	8.6
$r_{\rm s}$ [°]†	–	–	22.42	24.29
$T_{\rm s}/T$†	–	–	1.310	1.302
Σres^2	0.00125	0.00124	0.00130	0.00128

*"dark spot" on the primary star.
†"hot spot" on the secondary star.

figure 6. As shown in the left-hand panel, though these parameters provide very good light curve fittings for observations in 2014, they yield very bad light curve fittings for the observations in 2013, especially at the 0.25 and 0.75 phases. In this case a spotted model was used to re-analyze the light curves in 2013. The best fit was achieved under the assumption of a "dark spot" on the primary star and a "hot spot" on the secondary star. The corresponding theoretical light curves are also displayed in figure 6, in the right-hand panel. Clearly, compared with the light curves calculated without taking spots into account in the left-hand panel, the spotted parameters are much better for modeling the observations in 2013. The photometric parameters are listed in table 3.

Comparing the solutions from tables 2 and 3, the system's basic parameters derived by spotted models from the analysis of the 2013 light curves in table 3 are well matched with those of the 2014 light curves listed in table 2. This means that the high degree of asymmetry in the 2013 light curves can be explained by the presence of such active spotted regions. However, it is noted that all the derived solutions indicate that a third body contributes more than 60% of the total light of the system. This suggests that the color indices should primarily reflect the temperature of the third body. Thus the uncertainty in T_1 would be greater than that estimated by the color indices above. If the color indices suggest that the third body has a spectral type of about K5–K9, then the binary components are probably M stars, assuming they are normal main sequence stars. Considering the similar system 1SWASP J234401.81−212229.1, which may be a triple system consisting of two M-type components and a third middle K dwarf (Koen 2014), we recalculated the two sets of light curves with $T_1 = 3300$ K. The solutions of this are listed in table 4, where one can see that these new solutions deviated little from our previous ones. Figure 7 shows the geometrical structure of J075102.

5 Discussion and conclusions

Based on our two sets of $R_{\rm c}I_{\rm c}$ light curves, the photometric solutions of the extremely short period binary J075102 were derived with the W-D code. The results indicate that J075102 is a deep overcontact binary system with a high fillout of $f \approx 96\%$, and a high mass ratio of 0.70–0.78. This short-period contact binary is an A subtype system, where

the hotter component is also the more massive one. The results also reveal the existence of a third body in the system, which contributes more than 60% of the total light of the system. As mentioned above, there is a visual companion star near J075102, within about 4″, which our telescope can not resolve. Thus the visual companion contributes considerable parts of light to our light curves. However, as shown in the lower panel of figure 1, the visual companion is surely fainter than J075102, hence it is impossible that more than 60% of the total luminosity comes from the visual companion. In other words, J075102 is probably a triple system. The high degree of asymmetry in the 2013 light curves were well modeled by the existence of a "cool spot" on the primary component and a "hot spot" on the secondary component, the corresponding photometric parameters of which are in total agreement with those derived without a spotted model based on the symmetric light curve in 2014.

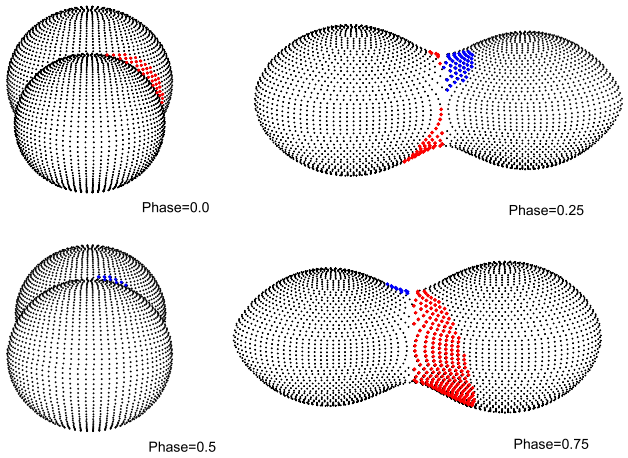

Fig. 7. Geometrical structure of J075102 with spots at phases 0.0, 0.25, 0.5, and 0.75. The blue areas refer to the "hot spot" on the secondary star and the red areas refer to the "dark spot" on the primary star. (Color online)

By using the classic $O-C$ method, the orbital period was analyzed. It was found that the $O-C$ diagram shows a long-term period increase [$dP/dt = +1.35(\pm 0.35) \times 10^{-7}$ d yr^{-1}]. This may be caused by a mass transfer from the less massive component to the more massive one. However, since the photometric solutions reveal that a third light exists in the system, we like to think the upward parabolic variation is a part of a cyclic variation, which is due to the light travel time effect of the third body. Also, as we know, the time scale of the angular momentum loss for these late type components is too long to reach contact phase within the age of the universe (Stępień 2006, 2011); thus a natural explanation for their existence would be that the close-in stellar companion had played an important role in their formation and evolution by extracting angular momentum from the central system (Qian et al. 2015).

As a newly discovered short-period contact system, J075102 displays many unusual features. In order to compare those properties with other similar systems, we have collected all the well-studied contact binaries with periods less than 0.23 d. Their parameters are listed in table 5. The results show that J075102 is one of the few A subtype systems with an extremely high fill-out of $f \approx 96\%$, while most of the others are in shallow contact, except for GSC1387−0475, which is also an overcontact binary with a high fill-out of $f \approx 76\%$. The system J075102 shows notable asymmetric and/or distorted light curves, which is a good indicator of strong surface activity in stars of this

Table 5. Sample of contact binaries with periods of less than 0.23 d.

Name	Period (d)	Subtype	q (or $1/q$)	f^* (%)	$L_3/L_{\rm total}$ (%)	M_3 ($M_\odot$)	Asym†	References‡
CC Com	0.220686	W	0.527	4.4–18	–	0.066	Yes	(1)–(7)
GSC 1387-0475	0.217811	A	0.474	76.3	33	∼0.47	No	(8), (9)
1SWASP J234401.81−212229.1	0.213676	W	0.422	20	80§	0.7	Yes	(10)–(12)
1SWASP J160156.04+202821.6	0.226529	W	0.67	10	–	–	Yes	(13)
SDSS J001641−000925	0.198561	A	0.62	18–25	–	$0.144/\sin i'$	No	(14), (15)
NSVS 4484038	0.218551	W	0.36	10	–	–	Yes	(16)
ASAS J071829−0336.7	0.2112594	W	0.65	0	–	–	Yes	(17)
1SWASP J074658.62+224448.5	0.220850	W	0.38	8.2	–	–	Yes	(18)
2MASS 02272637+1156494	0.21095	W	0.464	10.4	–	–	Yes	(19)
1SWASP J075102.16+342405.3	0.20917217	A	0.70–0.78	∼95	∼60	–	Yes	Present paper

*Degree of contact.

†Noticeable asymmetries were found in their light curves.

‡References: (1) Linnell and Olson (1989); (2) Qian (2001); (3) Yang and Liu (2003); (4) Pribulla et al. (2007); (5) Yang et al. (2009); (6) Zola et al. (2010); (7) Köse et al. (2011); (8) Rucinski and Pribulla (2008); (9) Yang, Wei, and Li (2010); (10) Lohr et al. (2012); (11) Lohr et al. (2013b); (12) Koen (2014); (13) Lohr et al. (2014); (14) Davenport et al. (2013); (15) Qian et al. (2015); (16) Zhang et al. (2014); (17) Pribulla, Vanko, and Hambalek (2009); (18) Jiang et al. (2015); (19) Liu et al. (2015).

§The value is average.

type. If this is the case, all those properties make J075102 a very important source among late-type contact binaries. Of course, to check these conclusions, new multicolor photometric and spectroscopic observations, as well as detailed investigations, are required in the future.

Acknowledgement

This work is supported by the Chinese Natural Science Foundation (Grant Nos. 11133007 and 11325315), the Strategic Priority Research Program "The Emergence of Cosmological Structure" of the Chinese Academy of Sciences (Grant No. XDB09010202), and the Science Foundation of Yunnan Province (Grant No. 2012HC011). New CCD photometric observations of the system were obtained with the 85 cm and 2.16 m telescopes at the Xinglong Station of National Astronomical Observatories of China and the 1 m telescopes at the Yunnan Observatories. The authors would like to thank Professor Marcus Lohr at the Open University for sending us their eclipsing timings of some short-period eclipsing binary candidates, and many thanks are due to Professor Andrew Norton at the Astrophysics Education department of the Royal Astronomical Society for providing us the data of SuperWASP.

References

Cox, A. N. 2000, Allen's Astrophysical Quantities, 4th ed. (New York: Springer)
Davenport, J. R. A., et al. 2013, ApJ, 764, 62
Jiang, D., Han, Z., Ge, H., Yang, L., & Li, L. 2012, MNRAS, 421, 2769
Jiang, L.-Q., Qian, S.-B., Zhang, J., & Zhou, X. 2015, AJ, 149, 169
Koen, C. 2014, MNRAS, 441, 3075
Köse, O., Kalomeni, B., Keskin, V., Ulaş, B., & Yakut, K. 2011, Astron. Nachr., 332, 626
Linnell, A. P., & Olson, E. C. 1989, ApJ, 343, 909
Liu, L., Chen, W. P., Qian, S. B., Chuang, R. J., Jiang, L. Q., Lin, C. S., & Hsiao, H. Y. 2015, AJ, 149, 111
Lohr, M. E., Hodgkin, S. T., Norton, A. J., & Kolb, U. C. 2014, A&A, 563, A34
Lohr, M. E., Norton, A. J., Kolb, U. C., & Boyd, D. R. S. 2013b, A&A, 558, A71
Lohr, M. E., Norton, A. J., Kolb, U. C., Anderson, D. R., Faedi, F., & West, R. G. 2012, A&A, 542, A124
Lohr, M. E., Norton, A. J., Kolb, U. C., Maxted, P. F. L., Todd, I., & West, R. G. 2013a, A&A, 549, A86
Pribulla, T., Rucinski, S. M., Conidis, G., DeBond, H., Thomson, J. R., Gazeas, K., & Ogłoza, W. 2007, AJ, 133, 1977
Pribulla, T., Vanko, M., & Hambalek, L. 2009, IBVS, 5886, 1
Qian, S.-B. 2001, Ap&SS, 278, 415
Qian, S.-B., et al. 2015, ApJ, 798, L42
Qian, S.-B., Jiang, L.-Q., Zhu, L.-Y., Zejda, M., Mikulášek, Z., Fernández-Lajús, E., & Liu, N.-P. 2014, Contrib. Astron. Obs. Skalnaté Pleso, 43, 290
Rucinski, S. M. 1992, AJ, 103, 960
Rucinski, S. M. 2007, MNRAS, 382, 393
Rucinski, S. M., & Pribulla, T. 2008, MNRAS, 388, 1831
Stepien, K. 2006, Acta Astron., 56, 347
Stępień, K. 2011, Acta Astron., 61, 139
Van Hamme, W., & Wilson, R. E. 2007, ApJ, 661, 1129
Wilson, R. E. 1979, ApJ, 234, 1054
Wilson, R. E. 1990, ApJ, 356, 613
Wilson, R. E. 2008, ApJ, 672, 575
Wilson, R. E. 2012, AJ, 144, 73
Wilson, R. E., & Devinney, E. J. 1971, ApJ, 166, 605
Wilson, R. E., Van Hamme, W., & Terrell, D. 2010, ApJ, 723, 1469
Yang, Y., & Liu, Q. 2003, PASP, 115, 748
Yang, Y.-G., Lü, G.-L., Yin, X.-G., Zhu, C.-H., & Nakajima, K. 2009, AJ, 137, 236
Yang, Y.-G., Wei, J.-Y., & Li, H.-L. 2010, New Astron., 15, 155
Zhang, X. B., et al. 2014, AJ, 148, 40
Zola, S., Gazeas, K., Kreiner, J. M., Ogloza, W., Siwak, M., Koziel-Wierzbowska, D., & Winiarski, M. 2010, MNRAS, 408, 464